Ecological controls on net ecosystem productivity of a mesic arctic tundra under current and future climates

R. F. Grant,[1] E. R. Humphreys,[2] P. M. Lafleur,[3] and D. D. Dimitrov[1,4]

Received 23 September 2010; revised 24 November 2010; accepted 22 December 2010; published 18 March 2011.

[1] Changes in arctic C stocks with climate are thought to be caused by rising net primary productivity (NPP) during longer and warmer growing seasons, offset by rising heterotrophic respiration (R_h) in warmer and deeper soil active layers. In this study, we used the process model *ecosys* to test hypotheses for these changes with CO_2 and energy fluxes measured by eddy covariance over a mesic shrub tundra at Daring Lake, Canada, under varying growing seasons. These tests corroborated substantial rises in NPP, smaller rises in R_h, and, hence, rises in net ecosystem productivity (NEP) from 17 to 45 g C m^{-2} yr^{-1} (net C sink), modeled with higher T_a and longer growing seasons. However, NEP was found to decline briefly during midsummer warming events (T_a > 20°C). A model run under climate change predicted for Daring Lake indicated that rises in NPP would exceed those in R_h during the first 100 years, causing NEP to rise. Rises in NPP were driven by more rapid net N mineralization from more rapid R_h in warming soils. However, greater declines in NEP were modeled during more frequent and intense midsummer warming events as climate change progressed. Consequently, average annual NEP (± interannual variability) rose from 30 (±13) g C m^{-2} yr^{-1} under current climate to 57 (±40) g C m^{-2} yr^{-1} after 90 years but declined to 44 (±51) g C m^{-2} yr^{-1} after 150 years, indicating that gains in tundra NEP under climate change may not be indefinite.

Citation: Grant, R. F., E. R. Humphreys, P. M. Lafleur, and D. D. Dimitrov (2011), Ecological controls on net ecosystem productivity of a mesic arctic tundra under current and future climates, *J. Geophys. Res.*, *116*, G01031, doi:10.1029/2010JG001555.

1. Introduction

[2] The soil organic carbon (SOC) within the top 1 m of arctic tundra is estimated to be 12%–25% of the global total, or about 500 Gt [*Tarnocai et al.*, 2009]. This SOC stock has accumulated slowly under the historically low temperatures, frequently saturated soils, and short growing seasons in the arctic, but may be changing more rapidly under climate warming currently in progress [*Polyakov et al.*, 2002]. However, the direction and rate of this change are determined by complex interactions among several key ecosystem processes affected by climate, and so remain unclear.

[3] Changes in SOC with climate are caused by changes in net primary productivity (NPP) versus heterotrophic respiration (R_h), differences between which cause changes in net ecosystem productivity (NEP). In upland arctic ecosystems, warming increases the duration, depth and temperature of the soil active layer, lowering the water table and increasing soil aeration, thereby raising R_h. If this rise exceeds that of NPP caused by the direct effects of warming duration and intensity on CO_2 fixation, NEP would decline and arctic ecosystems would become smaller sinks or greater sources of atmospheric CO_2. Such a decline would further raise atmospheric CO_2 concentrations (C_a) and the warming that rising C_a is thought to cause [*Oechel and Vourlitis*, 1994]. However, warming may further raise NPP by accelerating mineralization [*Chapin et al.*, 1995; *Weintraub and Schimel*, 2005] and hence plant N uptake, thereby alleviating N constraints on CO_2 fixation [*Sitch et al.*, 2007]. Consequently the rise in NPP from climate warming could exceed that in R_h, increasing NEP and causing arctic ecosystems to become greater sinks of atmospheric CO_2. Rising C_a may also increase NPP during climate warming, but only if sustained by more rapid nutrient uptake from accelerated mineralization [*Oechel et al.*, 1994]. Rising C_a may also affect NPP and R_h by reducing canopy stomatal conductance (g_c), thereby slowing transpiration and soil drying [e.g., *Grant et al.*, 2001].

[4] The sensitivity of arctic NEP to short-term changes in climate is apparent in the large interannual variability of NEP measured in eddy covariance (EC) studies. At some EC sites, NEP has been found to increase with the length and warmth of the growing season, largely determined by the timing of snowmelt and spring warming. These sites include a mixed mesic heath/shrub-hummock tundra in

[1]Department of Renewable Resources, University of Alberta, Edmonton, Alberta, Canada.
[2]Department of Geography, Carleton University, Ottawa, Ontario, Canada.
[3]Department of Geography, Trent University, Peterborough, Ontario, Canada.
[4]Now at Canadian Forest Service, Edmonton, Alberta, Canada.

Copyright 2011 by the American Geophysical Union.
0148-0227/11/2010JG001555

Canada [*Lafleur and Humphreys*, 2008], high arctic heaths in Greenland [*Groendahl et al.*, 2007] and Svalbard [*Lloyd*, 2001], and a subarctic fen in Finland [*Aurela et al.*, 2004]. However, increases in NEP with warming have not been found at other sites. Warmer and drier seasons reduced NEP of a moist tussock tundra and had little effect on NEP of a wet sedge tundra in Alaska [*Kwon et al.*, 2006].

[5] These contrasting responses of NEP to warming found in EC studies have been generally corroborated by those found in artificial warming experiments using open-top chambers (OTC) in Canada and Alaska. Warming raised gross primary productivity (GPP) and ecosystem respiration (R_e) in most of these experiments [*Oberbauer et al.*, 2007]. However, rises in R_e with warming were generally greater than those of GPP at drier sites, where below-ground R_e was stimulated by greater soil warming, than at wetter sites, where below-ground R_e was limited by poor aeration. Thus OTC warming reduced NEP of moist tussock tundra but raised that of wet sedge tundra in Alaska [*Oberbauer et al.*, 2007]. However, in the Canadian high arctic OTC warming raised NEP of dry and mesic sites, while reducing that of a wet site [*Welker et al.*, 2004]. Warming effects on NEP are therefore likely to depend on interactions among site conditions, landscape hydrology and climate.

[6] The EC and OTC studies of arctic NEP were confined in most cases to short summer growing seasons (typically June through August) and excluded autumn, winter and spring thaw seasons during which tundra ecosystems are net sources of CO_2 [*Fahnestock et al.*, 1999; *Laurila et al.*, 2001; *Oechel et al.*, 1997]. Carbon losses during these seasons can substantially offset C gains during summer when determining annual NEP [e.g., *Aurela et al.*, 2004; *Nobrega and Grogan*, 2007; *Welker et al.*, 2004]. Interannual variability in these losses appears to be smaller than that in C gains during summer [*Aurela et al.*, 2004]. However, the effect of climate change on C losses outside the growing season, and hence on annual NEP, remains largely unknown.

[7] Comprehensive studies of climate change effects on arctic NEP must also account for substantial amounts of CH_4 emitted from wetter ecosystems [e.g., *Christensen et al.*, 1996]. Changes in these emissions with climate will depend on the contrasting effects of soil warming, which raises emissions, and drying, which suppresses them. In some climate change projections, increased CH_4 emissions contribute substantially to CO_2-equivalent greenhouse gas emissions from the arctic [*Grant et al.*, 2003; *Zhuang et al.*, 2006]. These studies should also account for possible losses of dissolved organic C (DOC), especially if precipitation rates rise with climate change.

[8] The complexity of weather effects on arctic NEP favors the use of process models to test hypotheses for these effects under current climate, and to predict these effects under climate change. Predictions from some earlier modeling studies indicate that rises in NPP from warmer and longer growing seasons under higher C_a will be offset by rises in R_h from warmer soils, causing little change or small declines in NEP from current values [*Euskirchen et al.*, 2009; *Grant et al.*, 2003; *Zhuang et al.*, 2006]. However, predictions from other modeling studies indicate that rises in NPP will exceed those in R_h for part of the 21st century, allowing NEP to rise, although this rise may not be sustained later in the century [*Qian et al.*, 2010]. Uncertainty about the response of GPP to increasing C_a during climate change is the largest single factor contributing to uncertainty in these predictions [*McGuire et al.*, 2009; *Zhuang et al.*, 2006]. However, these predictions are also affected by other processes either omitted or not fully considered in the models, such as coupled C-N transformations, decomposition kinetics of SOC pools differing in lability, permafrost and snow hydrology and their effects on soil temperature (T_s) and C cycling, and changes in land use and disturbances [*Qian et al.*, 2010; *Sitch et al.*, 2007].

[9] In this study, we use the process model *ecosys* [*Grant*, 2001] to study the effects of short-term changes in weather and long-term changes in climate on net CO_2 and CH_4 exchange in a mesic tundra ecosystem. *Ecosys* is among the more complex and detailed models used in climate change studies. This model has been tested for response of CO_2 exchange to elevated C_a with Free Air CO_2 Enrichment (FACE) experiments [*Grant et al.*, 1995a, 1995b, 1999, 2001, 2004] and for response of CO_2 and CH_4 exchange to changes in weather and climate from eddy covariance (EC) measurements [e.g., *Grant and Roulet*, 2002; *Grant et al.*, 2003, 2007a, 2007b, 2008, 2009, 2010a] at hourly, daily, seasonal, annual and decadal time scales. Testing across this entire range of time scales is a vital prerequisite for modeling the projected impact of climate change on ecosystem productivity, which is expected to be caused by changes in short-term (diurnal and seasonal) variation of temperature and precipitation, as much as by rises in long-term (yearly and decadal) means. *Ecosys* has been used to predict the impact of climate change on productivity in several agricultural [*Grant et al.*, 2004], forest [*Grant and Nalder*, 2000; *Grant et al.*, 2006, 2007a, 2007b], tundra [*Grant et al.*, 2003] and grassland [*Li et al.*, 2004] ecosystems. The model is fully prognostic for all plant attributes used for resource acquisition in multiple canopy and soil layers (e.g., leaf area, root length), and thus simulates interactions between resource acquisition and growth by diverse plant functional types growing under specified site conditions (topography, soil, climate, disturbance).

[10] Based on earlier studies of arctic NEP, we hypothesize that (1) at an annual time scale, both NPP and R_h of mesic arctic tundra increase in years with earlier snowmelt and spring warming and decrease in those with later, (2) interannual variability in NPP caused by earlier or later warming is greater than that in R_h and so drives interannual variability in NEP, (3) at a daily time scale however, midsummer warming events may raise R_h more than NPP and thereby lower NEP, (4) if hypotheses 1 and 2 are supported, then at a decadal time scale climate change should raise average values and interannual variability of NPP more than those of R_h, thereby raising average values and interannual variability of NEP, and (5) if hypothesis 3 is supported, then rises in NEP with climate change may at some future point in time start to decline as midsummer warming events become more frequent and intense.

[11] To test hypotheses 1, 2 and 3, algorithms for weather effects on CO_2 and energy exchange in *ecosys* were compared with EC CO_2 and energy fluxes recorded over a mesic tundra at Daring Lake, Northwest Territories (NWT), Canada [*Lafleur and Humphreys*, 2008] during growing seasons differing in T_a and precipitation from 2004 to 2007. *Ecosys*

Table 1. Key Attributes of Vegetation, Soils, and Climate Within the EC Flux Tower Fetch at Daring Lake, NWT, Used in *ecosys*

	Attributes
Latitude N	64.9
Longitude W	111.6
Aspect (°)	160
Slope (°)	2.4
Plant functional types	evergreen and deciduous shrubs, sedges
Surface organic layer depth (cm)	6.5
Surface organic layer C:N	30
Mineral soil texture	sand to loamy sand
Mineral soil C:N (0–50 cm)	25
Period of measurement	2004–2007
MAT (°C)	−10.0 to −12.5
Precipitation (mm yr^{-1})	200–300
Recent site references	*Lafleur and Humphreys* [2008]

was then used to examine hypothesis 4 and 5 at daily, annual, decadal and centennial time scales under climate change predicted for the Daring Lake area.

2. Methods

2.1. Site Description

[12] The study site was located near Daring Lake in the central NWT of Canada (64°52.131′N, 111°34.498′W) about 300 km northeast of Yellowknife and 70 km north of the tree line. The site was described in detail by *Lafleur and Humphreys* [2008], and by *Nobrega and Grogan* [2007, 2008], so that a summarized description is given here. The landscape was treeless tundra with exposed bedrocks and dense coverage of small lakes that occupied ~30% of the area. The long-term mean annual temperature was estimated to be between −10°C and −12.5°C [*Climatic Atlas of Canada*, 1984]. Snowmelt typically occurred between late May and early June. From 15 May to 31 August, the period during which EC measurements were made, mean monthly temperatures remained above 0°C and maximum monthly temperature in July varied between 12.5°C and 15°C. Annual precipitation ranged between 200 and 300 mm, of which 75–125 mm were received during June–August. Continuous permafrost extended to a depth of about 160 m [*Dredge et al.*, 1999] with a very shallow active layer that varied from 0.5 to 1.2 m depending on soil type and vegetation cover. Belowground C within the active layer was estimated to be 23 ± 4 kg C m^{-2}.

[13] Vegetation at the site consisted of typical mixed tundra plant communities that followed a moisture gradient driven by local topography. A mesic lichen-heath evergreen mat (*Ledum decumbens* (Ait.), *Vaccinium vitis-idaea* (L.), *Empetrum nigrum* (L.), *Loiseleuria procumbens* (L.)) dominated the highest local relief, along with deciduous shrubs (*Betula glandulosa* (Michx.), *Rubus chamaemorus* (L.), *Vaccinium uliginosum* (L.)), and some graminoids (*Carex* spp. (L.)), while moist shrub/sedge plant communities were found at lower elevations. The mesic lichen-heath mat had a very thin organic layer of <0.03 m, underlain by well-drained sand and unsorted gravel subsoils. The moist shrub/sedge tundra had a variable organic layer of 0.05 to 0.10 m depth below shrubs and 0.15 to 0.30 m depth below sedges. Shrubs and sedges occupied relatively drier and wetter patches, respectively. Average shrub height was 0.15–0.20 m, and peak leaf area index (LAI) was about 0.8 in the mesic heath tundra and 0.9 in the moist shrub/sedge tundra. Moss consisted mainly of *Sphagnum* species below shrubs and in sedge hollows. Moss coverage increased with increasing soil moisture downslope while lichen coverage decreased, averaging 28% and 55%, respectively, within the tower fetch area.

2.2. Site Measurements

[14] An EC flux tower and an auxiliary meteorological tower were established in May 2004 over a mixed mesic tundra 1 km east of the Daring Lake Terrestrial Ecological Research Station, NWT, Canada. The tower fetch had a 2.5% slope from NW to SE with a minimum length of 400 m in all directions. CO_2 and energy fluxes were recorded continuously from mid-May to late August or September each year from 2004 to 2007. Tower instrumentation and methodology are described by *Lafleur and Humphreys* [2008], including gap-filling protocols and corrections to CO_2 flux measurements made using an open-path infrared gas analyzer during snow covered periods in spring based on comparisons with closed-path measurements. Static surface flux chambers were used to measure CH_4 exchange at different sites within the tundra landscape [*Hayne*, 2009].

2.3. Model Development

[15] The key algorithms governing the simulation of NEP in *ecosys* are described in Text S1, in which equations and variables referenced in the text below are described and listed in Appendices A, B, C and D.[1] Algorithms representing biological processes (Appendices A, B, C) were solved at an hourly time step from hourly changes in atmospheric boundary conditions, while those representing physical processes (Appendix D) were solved at a 5 min time step assuming constant boundary conditions during each hour. All parameters remained unchanged from those in earlier studies of boreal forests [e.g., *Grant et al.*, 2003, 2006, 2007a, 2007b, 2008, 2009, 2010a] to test the robustness of model algorithms under a colder arctic climate, particularly that of temperature functions governing plant [C10, C22, C23] and microbial [A5, A19] process rates.

2.4. Model Experiment

[16] Site conditions were simulated by initializing *ecosys* with the biological properties of the key plant functional types, the physical and chemical properties of the soil, and the topographic properties of the landscape at the mesic mixed tundra site at Daring Lake (Table 1). The biological properties of the evergreen and deciduous shrubs which dominated the site were the same as those used for evergreen and deciduous trees in earlier modeling studies of boreal forests, but with greater branching and shortened internode lengths to reproduce the dwarf stature of the vegetation at Daring Lake. The biological properties of sedge were the same as those of grass [*Grant and Flanagan*, 2007], but with greater root porosity to function in wet soils. Moss and lichen were not included in the model PFTs

[1] Auxiliary materials are available in the HTML. doi:10.1029/2010JG001555.

Table 2. Changes in Seasonal Mean Solar Radiation, Maximum and Minimum Air Temperatures, and Precipitation Predicted From 2001–2010 to 2091–2100 by the CRCM Version 4.2 Grid Cell Within Which the Daring Lake Site Is Located[a]

	Change From Current Value (°C)		Ratio to Current Value	
Season	Max. Temp.	Min. Temp.	Precipitation	Solar Radiation
Dec–Feb	5.53	5.88	1.43	0.89
Mar–May	3.34	4.53	1.32	0.92
Jun–Aug	2.05	3.90	1.51	0.86
Sep–Nov	4.23	4.83	1.37	0.87

[a]The seasonal changes were calculated from Canadian Regional Circulation Model (CRCM) version 4.2 monthly data generated and supplied by the Ouranos Climate Simulation Team via the Canadian Climate Centre for Modeling and Analysis (CCCMA) data distribution web page.

because moss was present only in parts of the tower fetch, and lichen is not currently modeled in *ecosys*. The model was then run during model years 1901 to 2007 under repeating sequences of continuous hourly weather data (radiation, T_a, dew point or RH, wind speed and precipitation) recorded at Daring Lake from 1 January 2004 to 31 December 2007. These data were recorded at the field site from 15 May to 31 August each year, and at the Daring Lake Tundra Ecological Research Station (TERS), located about 250 m from the field site, during the rest of the year. Winter precipitation was calculated from hourly gains in snowpack depth measured by a sonic sensor at TERS assuming a bulk density of 0.083 Mg m^{-3}, reduced by declines in snowpack depth attributed to wind. The repeating weather sequence in the model run was 6 years in length, starting with two consecutive 2005 years to provide meteorologically near-average weather prior to the continuous 2004–2007 weather sequence.

[17] Plant functional types were seeded during the first year of the model run, but were not disturbed thereafter. The presence of permafrost in the model prevented drainage through the lower boundary of the soil, but surface runoff [D1–D6] was allowed to leave freely in order to simulate the hydrology of the mesic mixed tundra site. During the model run, C_a rose exponentially from 280 μmol mol^{-1} to 385 μmol mol^{-1}, NH_4^+ and NO_3^- concentrations in precipitation used to simulate wet deposition were both maintained at 0.3 g N m^{-3} [*Meteorological Service of Canada*, 2004], and NH_3 concentration in the atmosphere used to simulate dry N deposition was maintained at 0.0025 μmol mol^{-1}.

2.5. Model Testing

[18] CO_2 and energy exchange simulated by *ecosys* during model years 2004 to 2007 were compared at hourly, daily and seasonal time scales with those measured at the EC flux tower over the mixed tundra site at Daring Lake from 2004 to 2007, and gap filled as described by *Lafleur and Humphreys* [2008]. Model performance in each year was evaluated from regressions of modeled hourly CO_2 and *LE* fluxes on measured hourly averaged EC CO_2 and *LE* fluxes in which both half-hourly values were considered accurate. Evaluations were based on intercepts ($a \rightarrow 0$), slopes ($b \rightarrow 1$), correlation coefficients ($R^2 \rightarrow 1$), and on comparisons of root mean squares for differences between EC and modeled fluxes (RMSD) versus estimated root mean squares for error in EC fluxes (RMSE). Values of RMSE for each year were calculated as the pooled root mean square of uncertainty in half-hourly EC fluxes during the year using equations for CO_2 random flux measurement errors derived over vegetation of comparable stature by *Richardson et al.* [2006].

2.6. Model Projections

[19] A climate change projection for Daring Lake was derived from the Canadian Regional Circulation Model (CRCM) v.4.2.3 time slice simulation for 1961–2100 driven by Canadian General Circulation Model (CGCM) v.3, following the IPCC "observed twentieth century" scenario for years 1961–2000 and the SRES A2 scenario for years 2001–2100. This simulation was conducted over the North American domain with a 45 km horizontal grid-size mesh [*Music and Caya*, 2007]. Differences in mean monthly values for solar radiation, maximum and minimum T_a, and precipitation (snow + rain) between those averaged over 2001–2010 and those over 2091–2100 were calculated for the model grid cell in which the Daring Lake site was located (Table 2). These differences were calculated as hourly values and applied to the repeated sequences of hourly weather data recorded from 2004 to 2007 at Daring Lake during a continuation from model years 2008 to 2157 of the model run described under *Model Testing*. These hourly changes allowed the current climate to transition to the predicted one over a realistic time frame while maintaining the short-term variability in weather that governs CO_2 and energy exchange. Such transition is important in climate change studies because different time lags among the responses of diverse ecosystem processes to climate change may complicate the modeling of long-term changes from short-term mechanisms [*Chapin and Shaver*, 1996]. NEP and ecosystem C stocks modeled from 2004 to 2007 were contrasted with those modeled as climate change progressed during model years 2008 to 2097, the period of the CRCM climate change projection, and extrapolated for a further 60 years assuming that climate change continued at the same rate.

3. Results

3.1. Current Climate

3.1.1. Tests of Modeled Versus Measured CO_2, CH_4, and LE Fluxes

[20] Regressions of modeled on measured hourly CO_2 fluxes during each year from 2004 to 2007 indicated an absence of bias in the modeled results during the study period (intercept a close to zero, slope b close to one in Table 3), except during 2004 when modeled fluxes were larger. The absence of 2003 weather data caused some uncertainty in the 2004 fluxes because snowpack depth and T_s at the beginning of the year may not have been accurately simulated (Figure 1b). Modeled and measured CO_2 fluxes were sufficiently well correlated (R^2 from 0.7 to 0.8) that variation in the EC fluxes unexplained by the model (RMSD) was similar to random error estimated from the EC flux measurements using an algorithm developed by *Richardson et al.* [2006] (RMSE), or estimated as 20% of EC values by *Wesely and Hart* [1985]. However, modeled CO_2 fluxes tended to be larger than gap-filled values ($b > 1$ in Table 3), particularly in 2006.

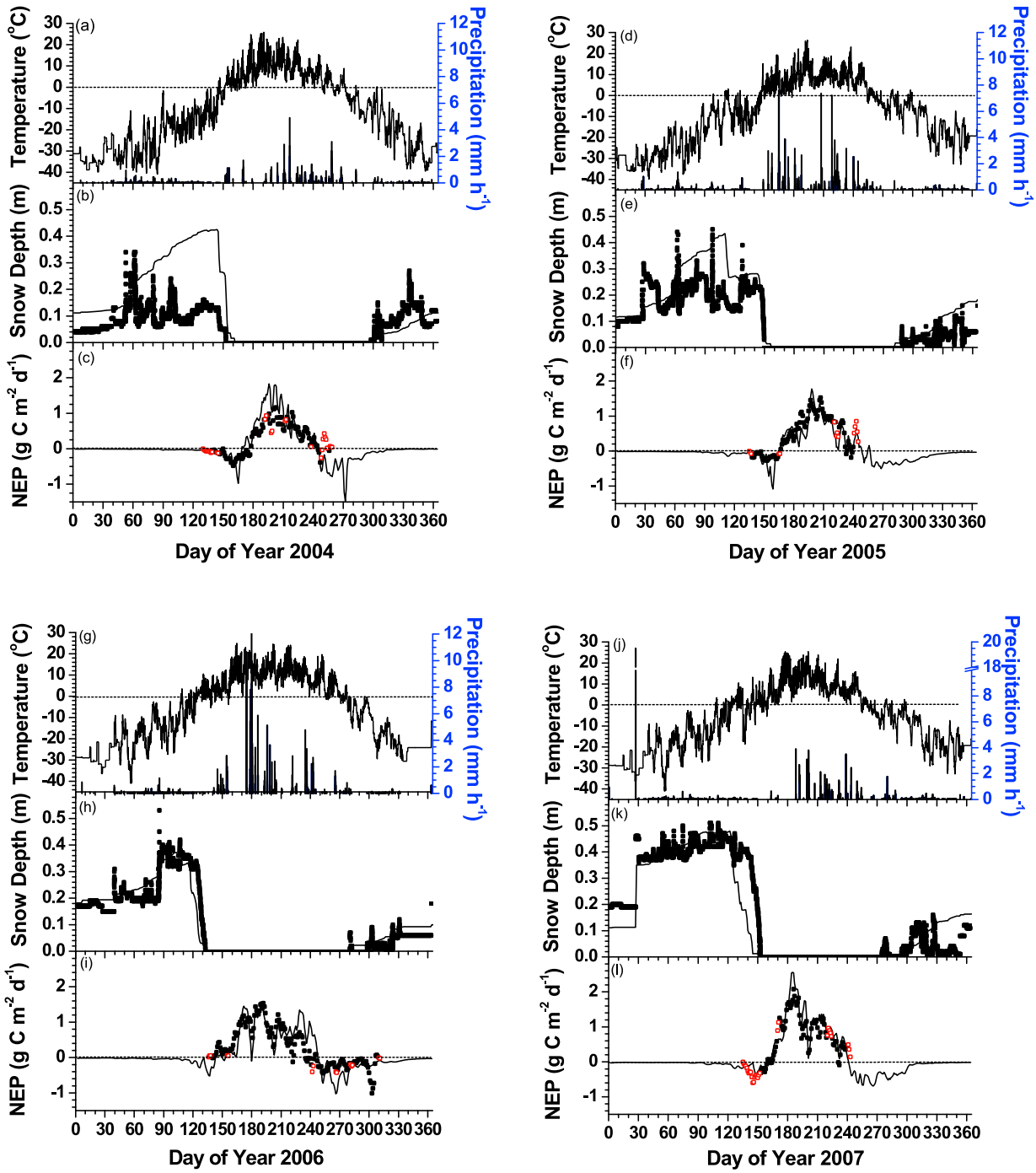

Figure 1. (a–l) Hourly air temperatures, precipitation, snowpack depths, and 3 day moving averages of daily net ecosystem productivity (NEP) measured (symbols) and modeled (lines) from 2004 to 2007 at Daring Lake NWT. Positive and negative values for NEP denote net C uptake and emission, respectively. Open symbols for NEP represent daily values consisting of more than 24 half-hourly gap-filled fluxes.

[21] Regressions of modeled on measured *LE* fluxes also indicated an absence of bias in the modeled results, except in 2005 when modeled fluxes were slightly smaller (Table 3). RMSD for *LE* fluxes from the regressions were similar in all years to RMSE estimated from the EC flux measurements using an algorithm developed by *Richardson et al.* [2006]. These values for RMSD from the regressions indicated that closer agreement between measured and modeled fluxes of CO_2 and *LE* was unlikely to be achieved without further reducing uncertainty in the EC measurements.

[22] Measurements of CH_4 fluxes in the mesic heath and shrub tundras that dominated the EC tower fetch indicated very slow uptake (mean summer values 0.5–0.8 nmol m^{-2} s^{-1}) [*Hayne*, 2009]. These fluxes were consistent with those modeled, annual totals of which remained within 0.001 g C m^{-2} of zero during each year of the study.

Table 3. Intercepts (*a*), Slopes (*b*), Coefficients of Determination (R^2), Root Mean Square of Differences Between Modeled and Measured Fluxes (RMSD), Root Mean Square of Error in Measured Fluxes (RMSE) Calculated for Vegetation of Comparable Stature From *Richardson et al.* [2006], and Number of Accepted Eddy Covariance (EC) Fluxes (*n*) From Regressions of Hourly Modeled Versus Measured and Gap-Filled CO_2 Fluxes and Measured *LE* Fluxes From 2004 to 2007 at Daring Lake, NWT[a]

Year	*a*	*b*	R^2	RMSD	RMSE	*n*
			Measured CO_2 Fluxes			
2004	0.19 μmol m^{-2} s^{-1}	1.13	0.74	0.59 μmol m^{-2} s^{-1}	0.59 μmol m^{-2} s^{-1}	1872
2005	0.00 μmol m^{-2} s^{-1}	1.05	0.77	0.63 μmol m^{-2} s^{-1}	0.61 μmol m^{-2} s^{-1}	1716
2006	0.05 μmol m^{-2} s^{-1}	1.02	0.69	0.74 μmol m^{-2} s^{-1}	0.62 μmol m^{-2} s^{-1}	2949
2007	0.22 μmol m^{-2} s^{-1}	1.03	0.78	0.79 μmol m^{-2} s^{-1}	0.69 μmol m^{-2} s^{-1}	1619
			Gap-Filled CO_2 Fluxes			
2004	−0.19 μmol m^{-2} s^{-1}	1.12	0.64	0.43 μmol m^{-2} s^{-1}		955
2005	−0.36 μmol m^{-2} s^{-1}	1.17	0.85	0.45 μmol m^{-2} s^{-1}		731
2006	−0.01 μmol m^{-2} s^{-1}	1.44	0.66	0.40 μmol m^{-2} s^{-1}		924
2007	−0.05 μmol m^{-2} s^{-1}	1.07	0.74	0.54 μmol m^{-2} s^{-1}		798
			Measured LE Fluxes			
2004	−0.6 W m^{-2}	1.00	0.73	22 W m^{-2}	28 W m^{-2}	1760
2005	−3.2 W m^{-2}	0.89	0.70	27 W m^{-2}	30 W m^{-2}	1733
2006	−0.1 W m^{-2}	1.03	0.81	19 W m^{-2}	27 W m^{-2}	3357
2007	−4.4 W m^{-2}	1.08	0.74	22 W m^{-2}	29 W m^{-2}	1570

[a]All measured fluxes are hourly averages of two accepted half-hourly values. Here *a*, *b*, and R^2 are from regressions of modeled on measured fluxes, and RSMD is from regressions of measured on modeled fluxes.

3.1.2. Annual Ecosystem Productivity Under Current Climate

[23] There was considerable interannual variation in weather that affected ecosystem productivity during the study period at Daring Lake. Temperatures and precipitation rose, spring thawing advanced, and autumn freezing was delayed from 2004 to 2006 (Table 4). Temperatures and precipitation then declined and spring thawing was delayed from 2006 to 2007. This variation caused rises from 2004 to 2006 and then small declines from 2006 to 2007 in modeled GPP [C1, C6, C7, C10], autotrophic respiration (R_a) [C13, C22, C23], NPP (= GPP − R_a), R_h [A11, A5, A19], and ecosystem respiration (R_e = R_a + R_h) (Table 4). Warming from 2004 to 2006 further raised R_h in the model by delaying autumn freezing (Table 4), and by increasing the maximum depth of the soil active layer from 0.7 to 0.9 m, although subsequent cooling advanced autumn freezing and reduced active layer depth to 0.7 m in 2007. Rises in GPP and R_e modeled from 2004 to 2006, and the small decline in R_e modeled from 2006 to 2007 corresponded to those in EC-derived values, although the small decline in GPP modeled from 2006 to 2007 was not found in the EC results. Interannual variation in GPP and R_e modeled and measured from 2004 to 2007 caused a rising trend in NEP (Table 4).

[24] Annual GPP and R_e from the model were greater than those derived from EC measurements (Table 4), although the modeled and measured CO_2 fluxes from which these values arose were in closer agreement (Table 3). The larger modeled versus EC-derived R_e and hence GPP could be partly attributed to larger modeled versus gap-filled CO_2 fluxes (Table 3), most of which were effluxes gap filled during nights when inadequate atmospheric turbulence required replacement of measured values.

[25] Warming from 2004 to 2006 increased both modeled and EC-derived GPP more than R_e, and therefore increased NEP, consistent with hypotheses 1 and 2. However, cooling from 2006 to 2007 reduced both modeled and EC-derived R_e more than GPP, and therefore increased NEP further. The greater decrease of R_e versus GPP in 2007 was attributed in the model to slower decomposition and hence R_h during drying of surface litter and underlying soil [A3, A4] under lower precipitation (Table 4). However, slower decomposition left more litter to drive R_h with later rewetting, so that this gain in NEP was short lived. The modeled and EC-derived NEP indicated that the mesic mixed tundra at Daring Lake was a net sink of 41–76 and 32–66 g C m^{-2}, respectively,

Table 4. Mean Temperature, Total Precipitation, Start of Spring Thaw and Autumn Freezing, Annual Carbon Balances, and Evapotranspiration Modeled or Derived From Eddy Covariance Measurements (EC) During the Growing Season, Represented by the EC Measurement Period Between 15 May and 31 August (*s*) or During the Entire Year (*y*) at Daring Lake, NWT, From 2004 to 2007

	2004		2005		2006		2007	
Weather	*s*	*y*	*s*	*y*	*s*	*y*	*s*	*y*
Temp. (°C)	6.3	−12.2	6.9	−8.9	10.2	−7.3	8.2	−9.5
Precipitation (mm)	72	155	159	224	248	288	84	155
Thaw (DOY)	162		155		133		150	
Freeze (DOY)	262		259		272		258	
C balance modeled[a]								
GPP	229	244	256	284	339	386	307	320
R_a	79	97	88	111	121	154	108	127
NPP	150	147	168	173	218	232	199	193
R_h	103	127	127	157	159	198	123	148
R_e	182	224	215	267	280	352	231	275
NEP	+47	+20	+41	+17	+59	+34	+76	+45
DIC, DOC[b]		0.7		0.6		0.5		0.6
ET (mm)	119	130	130	142	181	200	152	167
C balance EC[c]								
GPP	132		165		209		209	
R_e	100		114		148		143	
NEP	+32		+51		+61		+66	
ET (mm)	130		152		181		145	

[a]C balance is in g C m^{-2} $season^{-1}$ or g C m^{-2} yr^{-1}.
[b]Dissolved inorganic and organic C exported in runoff water.
[c]C balance is in g C m^{-2} $season^{-1}$ or g C m^{-2} yr^{-1}. From *Lafleur and Humphreys* [2008].

during 15 May to 31 August measurement periods from 2004 to 2007. However, R_e exceeded GPP modeled during the rest of the year, causing the tundra to be a net C source outside the measurement period. This source varied less from year to year (24–31 g C m^{-2}) than did the net C sink modeled during the measurement period (Table 4), so that annual NEP modeled for the mesic mixed tundra at Daring Lake varied from 17 to 45 g C m^{-2} yr^{-1} (Table 4).

3.1.3. Seasonal Ecosystem Productivity Under Current Climate

[26] The effects of warming on annual NEP modeled and measured during 2004–2007 (Table 4) arose from seasonal effects of temperature and precipitation on daily GPP, R_e and hence NEP (Figure 1). These effects arose in part from earlier snowmelt (Figures 1b, 1e, 1h, and 1k) and spring warming (Figures 1a, 1d, 1g, and 1j) that advanced the onset of net C uptake by evergreen and deciduous plant functional types from DOY 180 in 2004 to DOY 171 in 2005, DOY 158 in 2006 and DOY 167 in 2007 (Figures 1c, 1f, 1i, and 1l). In the model, the onset of net C uptake followed initiation of evergreen dehardening and deciduous leafout after a set number of hours accumulated above a set plant temperature under increasing day lengths, as described by *Grant et al.* [2008, 2009]. Deciduous leafout was modeled (observed) on DOY 165 (166) in 2004, DOY 158 (160) in 2005, DOY 146 (148) in 2006, and DOY 159 in 2007.

[27] Net C uptake declined more slowly during August in warmer years (e.g., 2006 and 2007 in Figures 1i and 1l) than in cooler years (e.g., 2004 and 2005 in Figures 1c and 1f). However, gains in NEP with warming were reversed by brief warming events (T_a > 20°C) that caused small declines in net C uptake during early summer (e.g., around DOY 190 of 2005 and DOY 175 of 2007 in Figures 1f and 1l), and much larger declines in net C uptake during midsummer (e.g., around DOY 200 of 2006 and 2007 in Figures 1i and 1l).

[28] Net C uptake modeled and measured during the growing season was partially offset by net C emissions modeled and measured during the rest of the year (Table 4), particularly during the months immediately preceding and following those of net C uptake (Figure 1). In the model, net C emissions were largely attributed to sustained R_h in surface litter and comparatively warm soil between deciduous leafoff at the end of August and sustained soil freezing in late October. Emissions modeled during this period were only partially offset by net C uptake from evergreen shrubs under declining T_a and day length. EC measurements through September and October 2006 also indicated sustained net C emissions (Figure 1i). Most of the seasonal variation in EC-derived daily NEP during 2004–2007 was simulated, except during early summer in 2004 (Figure 1c), likely due to the absence of recorded weather data during the previous model year. Losses of C from DOC export in the model remained small (Table 4).

3.1.4. Diurnal CO_2 and Energy Exchange Under Current Climate

[29] Changes in daily NEP resulted from diurnal changes in CO_2 influxes driven by GPP, and in CO_2 effluxes driven by R_a and R_h. The more rapid rise of net C uptake with earlier spring warming from 2004 to 2007 (Figure 1) was apparent in more rapid CO_2 influxes and effluxes modeled and measured during the onset of peak net C uptake in early July (e.g., DOY 182 to 188 in Figure 2). At this time of year, long day lengths (Figures 2a, 2e, and 2i) caused CO_2 influxes to continue during most of the day, with only 2–3 h of CO_2 effluxes around midnight (Figures 2d, 2h, and 2l), so that daily net C uptake rose rapidly after deciduous leafout in early June (Figure 1). Earlier spring warming, with less precipitation and greater solar radiation in 2006 and 2007 versus 2005 (Figures 2e and 2i versus Figure 2a), hastened leaf area growth [C21] and hence raised CO_2 influxes [C1] measured and modeled during early July (Figures 2f and 2j versus Figure 2b). Rises in CO_2 fixation with warming in the model were driven by those in canopy temperature (T_c) [C10] which rose several degrees above T_a because *LE* [B1] remained low with respect to net radiation (R_n), forcing sensible heat loss (*H*) through canopy warming (Figures 2c, 2g, and 2k). During 2007, soil drying caused by low spring precipitation (Figure 1j) forced lower soil and canopy water potentials in the model (ψ_s and ψ_c) [B14], hence lower g_c [B3, B4], lower *LE* versus *H* (Figure 2k; [B1], and earlier declines in afternoon CO_2 influxes (Figure 2l; [C2, C9].

[30] Earlier warming in 2006 versus 2005 also raised soil temperature (T_s) (Figure 2f versus Figure 2b) [D12], and hence CO_2 effluxes (Figure 2h versus Figure 2d) [A5, A19]. Drying of surface litter and underlying soil during early July 2007 lowered microbial decomposition rates in the model [A3, A4], and hence R_h [A13] and CO_2 effluxes (Figure 2h and Table 4), contributing to greater NEP (Figure 1l). Rises in CO_2 influxes with spring warming from 2005 to 2007 exceeded those in CO_2 effluxes, raising peak net C uptake in early summer (Figures 1i and 1l versus Figure 1f and Table 4), consistent with hypotheses 1 and 2. Modeled CO_2 effluxes exceeded gap-filled values, particularly in 2006 (Figure 2h and Table 3), contributing to larger modeled versus EC-derived R_e and GPP (Table 4). In the model, CO_2 effluxes were primarily driven by R_a of plant biomass grown from CO_2 fixation products at an hourly time scale [C13], and by R_h of plant litterfall and its decomposition products derived from plant biomass at seasonal to decadal time scales [A11]. Model coefficients used to calculate R_a and R_h from plant biomass and litterfall were well constrained from basic research [e.g., *Waring and Running*, 1998]. Therefore CO_2 effluxes in the model were not independent of CO_2 influxes, which were generally consistent with measured values (Table 3 and Figures 2 and 3), but rather were driven by these influxes over a range of time scales.

[31] Warming events (T_a > 20°C) later in July 2006 and 2007 versus 2005 raised CO_2 influxes less than CO_2 effluxes (e.g., DOY 197–203 in Figures 3e and 3l versus Figure 3a). Rises in modeled influxes were driven by more rapid CO_2 fixation with higher T_c [C10]. However, T_c rose several degrees above T_a to values at which, during warming events, modeled CO_2 fixation became less responsive to warming in arctic-adapted species. Higher T_c was modeled because *LE* [B1] remained low with respect to R_n, forcing heat loss through *H* (Figures 3c, 3g, and 3k). During particularly warm days following periods of low precipitation, rises in CO_2 fixation modeled with rises in T_c were offset by declines in CO_2 fixation modeled with declines in ψ_c [B14] and g_c [B3] under higher *D*, apparent in lower *LE* versus *H* and midafternoon declines in CO_2 influxes (e.g., DOY 198 and 199 in Figures 3k and 3l).

[32] During these warming events, increases in R_h and below-ground R_a were driven by increases in T_s (Figures 3b,

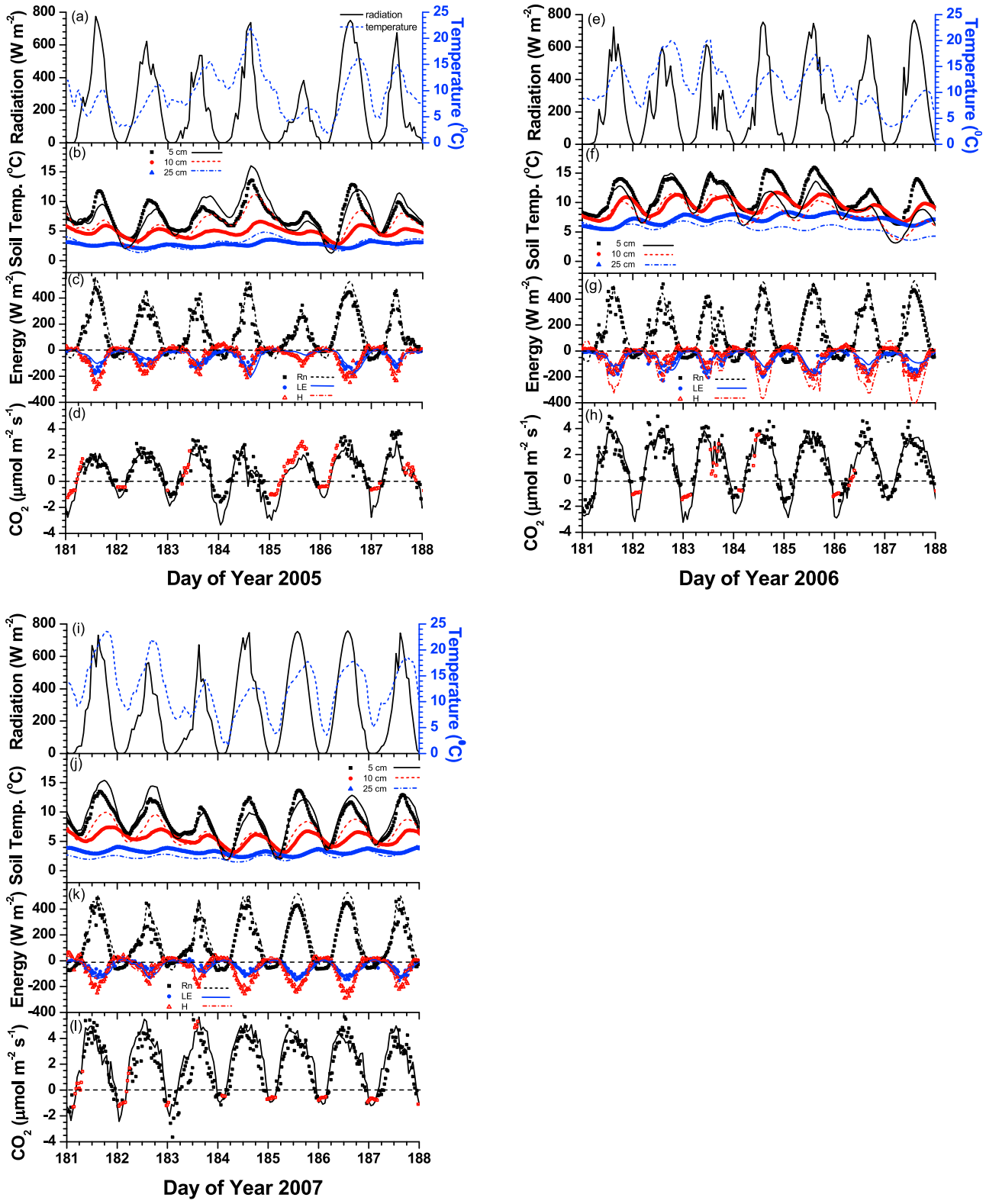

Figure 2. (a–l) Recorded solar radiation and air temperature and measured (symbols) and modeled (lines) soil temperature, energy, and CO_2 fluxes during DOY 182–188 from 2005 to 2007 at Daring Lake, NWT. Positive values denote downward fluxes, and negative values denote upward. Open symbols for CO_2 fluxes represent gap-filled values.

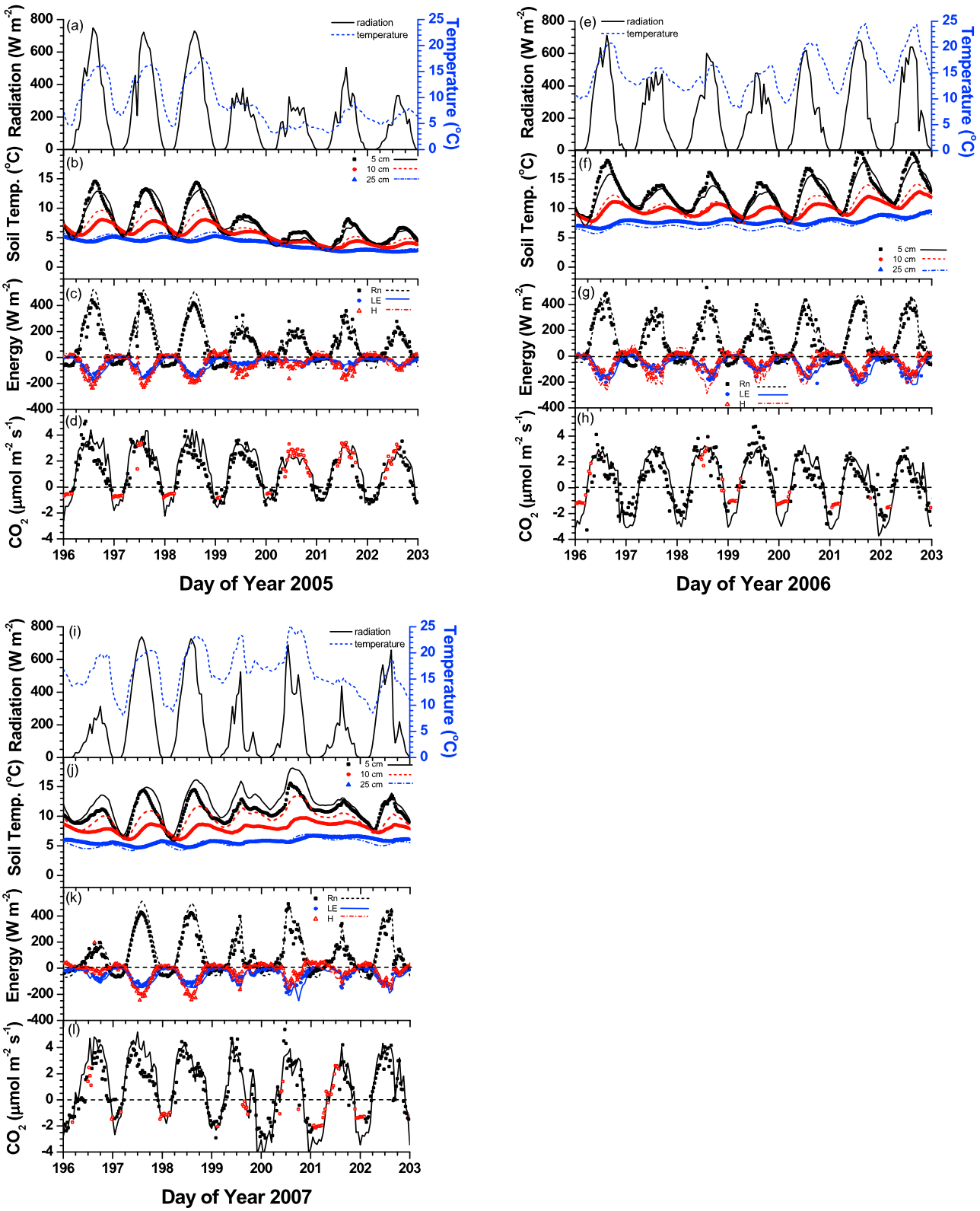

Figure 3. (a–l) Recorded solar radiation and air temperature and measured (symbols) and modeled (lines) soil temperature, energy, and CO_2 fluxes during DOY 197–203 from 2005 to 2007 at Daring Lake, NWT. Positive values denote downward fluxes, and negative values denote upward. Open symbols for CO_2 fluxes represent gap-filled values.

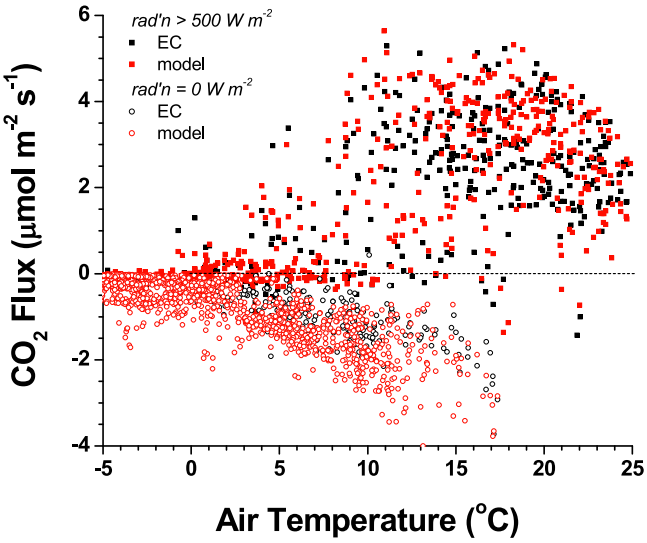

Figure 4. Functional relationships of air temperature with CO_2 flux measured by eddy covariance (EC) or modeled when solar radiation was greater than 500 W m^{-2} (solid symbols) or zero W m^{-2} (open symbols) at Daring Lake during 2007.

3f, and 3j) [D10]–[D12] through values at which R_h and R_a were very sensitive to warming [A5, C22]. Rapid rises in CO_2 effluxes modeled during DOY 200–202 in 2007 were driven by wetting of previously dry surface litter and soil from precipitation (Figure 1j), apparent in greater *LE* versus *H* (Figure 3k), which temporarily hastened microbial decomposition [A3, A4] and hence R_h. CO_2 influxes measured and modeled under nonlimiting irradiance were greatest when 10°C < T_a < 20°C, and declined when T_a > 20°C, while CO_2 effluxes measured and modeled under no irradiance rose continuously with T_a (e.g., during 2007 in Figure 4). Consequently CO_2 influxes rose little or even declined during these warming events, while CO_2 effluxes rose substantially (Figures 3h and 3l versus Figure 3d), causing brief but pronounced declines in daily NEP (Figure 1), supporting hypothesis 3.

3.2. Climate Change

3.2.1. Soil Hydrology and Temperature Under Climate Change

[33] Much of the climate change impact on NEP is thought to be effected through soil water content (θ) and T_s. The application of changes in radiation, T_a and precipitation derived from the CRCM v.4.2.3 climate change scenario to 2004–2007 weather caused modeled snowpacks to deepen (Figure 5a), and snowmelt and spring thawing (Figure 5b) [D8, D12] to advance by about one week after 90 years. Summer θ declined slightly during the first 30 years of climate change (Figure 5b), particularly during years incremented from drier 2007 weather (Figure 1j), but rose thereafter because rises in precipitation (Table 2) exceeded those in evapotranspiration (ET). Rises in ET were driven by the effects on *LE* of greater *D* from rising T_c [B1] but limited by those of lower g_c from rising C_a [B2], so that *LE* rose little during climate change (e.g., Figures 7c and 7g below). Autumn freezing [D8, D12] was delayed by up to two weeks as climate change progressed, gradually lengthening the growing season.

[34] Climate change caused T_s to rise (Figure 5c), particularly during winter when soil heat losses in the model were slowed by greater rises in T_a (Table 2) and by slower heat loss through deeper snowpacks (Figure 5a) [D10, D11] modeled under rising precipitation (Table 2). T_s rose earlier in spring and declined later in autumn, increasing both the duration and the warmth of the active layer (Figure 5b). Climate change also increased the maximum depth of the active layer from 0.8 to 1.1 m after 90 years. Rises in T_s during spring and summer, and declines during autumn and winter lagged those in T_a under climate change due to greater canopy shading [C21] and a thicker surface litter layer [D10–D12] generated by greater NPP modeled under rising T_a and C_a.

3.2.2. Net Ecosystem Productivity and Climate Change

[35] Increased warmth and duration of the growing season during climate change (Figures 5a, 5b, and 5c) caused increases in both the rate and duration of net C uptake as climate change progressed (e.g., from 2004–2007 to 2094–2097 in Figure 6). These increases were greatest during earlier spring warming in each year, as was modeled during earlier spring warming under current climate (e.g., from 2004 to 2007 in Figure 1). Increases in net C uptake during earlier spring warming under climate change were modeled because rises in CO_2 influxes from CO_2 fixation modeled under rising T_a [C10], C_a [C6] and LAI [C1] were greater than those in CO_2 effluxes from R_h [A5] and R_a [C22] modeled under rising T_s (e.g., from 2005 to 2095 in Figure 7d). These same processes caused greater rises in CO_2 influxes versus effluxes to be modeled with earlier spring warming under current climate, consistent with measurements (e.g., from 2005 to 2007 in Figure 2), so that support for hypotheses 1 and 2 under current climate suggests support for hypothesis 4 under climate change. Rises in CO_2 fixation modeled during climate change were further sustained by higher T_s and θ (Figure 5b) which enabled more rapid R_h [A3]–[A5] (Figures 7d and 7h), and hence more rapid net N and P mineralization [A25] (Figure 8), asymbiotic N_2 fixation [A26], and hence root N and P uptake [A36] which raised CO_2 fixation capacity [C6, C8].

[36] Although net C uptake generally rose with climate change, more intense warming events (T_a > 20°C) caused greater declines in net C uptake to be modeled during midsummer in warmer years, in some cases causing the tundra briefly to become a net C source (e.g., around DOY 200 in years incremented from 2006 or 2007 weather in Figure 6). During these events (e.g., Figure 7e), CO_2 influxes rose less than did CO_2 effluxes (e.g., Figure 7h) because CO_2 fixation responded less to further warming at higher values of T_c [C10] than did R_h [A5] and R_a [C22] to further warming at lower values of T_s, even though T_s rose slightly less with climate change than did T_a (Figures 7b and 7f versus Figures 7a and 7e). These same processes caused smaller rises in CO_2 influxes versus effluxes to be modeled during warming events under current climate, consistent with EC measurements (Figures 3 and 4), so that support for hypothesis 3 under current climate suggests support for hypothesis 5 under climate change. Modeled CO_2 fixation

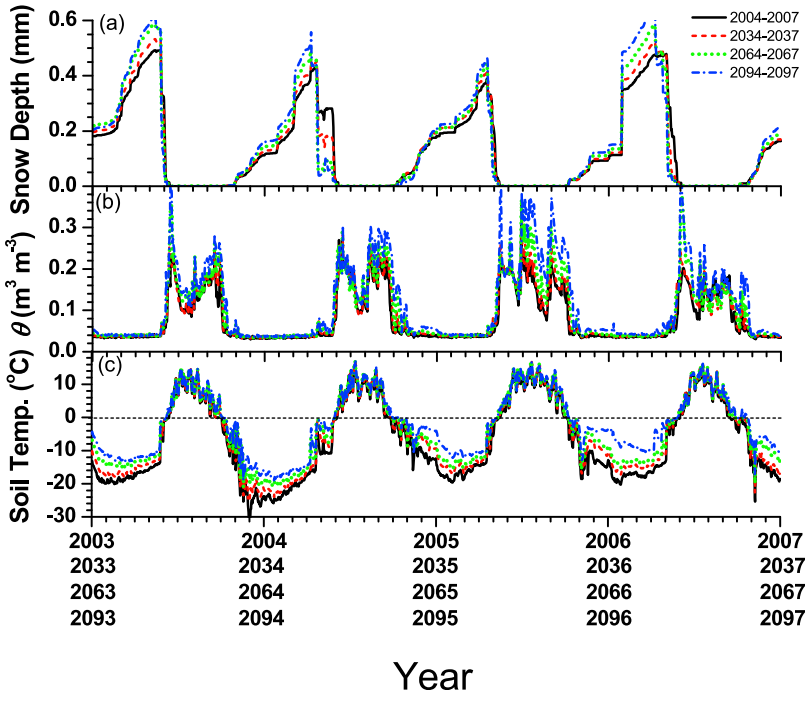

Figure 5. (a) Snowpack depth, (b) soil liquid water contents, and (c) soil temperatures simulated at 5 cm during 4 year periods at 30 year intervals from a 150 year model run under repeating sequences of weather data recorded at Daring Lake from 1 January 2004 to 31 December 2007. Weather data were altered hourly during model years 2008 to 2157 according to climate change predicted by the Canadian Regional Circulation Model (CRCM) version 4.2 grid cell within which the Daring Lake site is located (see Table 2).

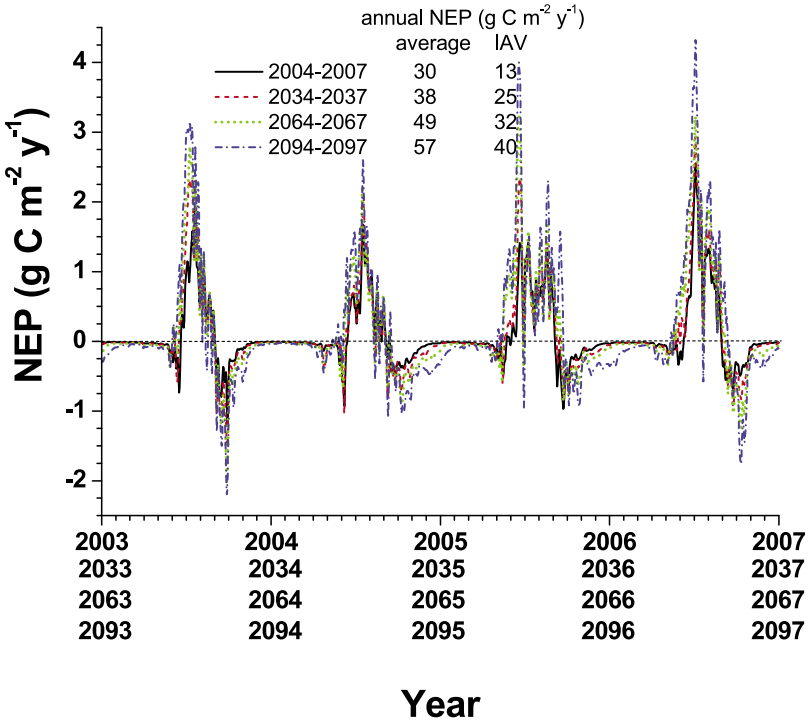

Figure 6. Net ecosystem productivity (NEP) during 4 year periods at 30 year intervals from a 150 year model run under repeating sequences of weather data recorded at Daring Lake from 1 January 2004 to 31 December 2007. These weather data were altered hourly during model years 2008 to 2157 according to climate change predicted by the Canadian Regional Circulation Model (CRCM) version 4.2 grid cell within which the Daring Lake site is located (see Table 2).

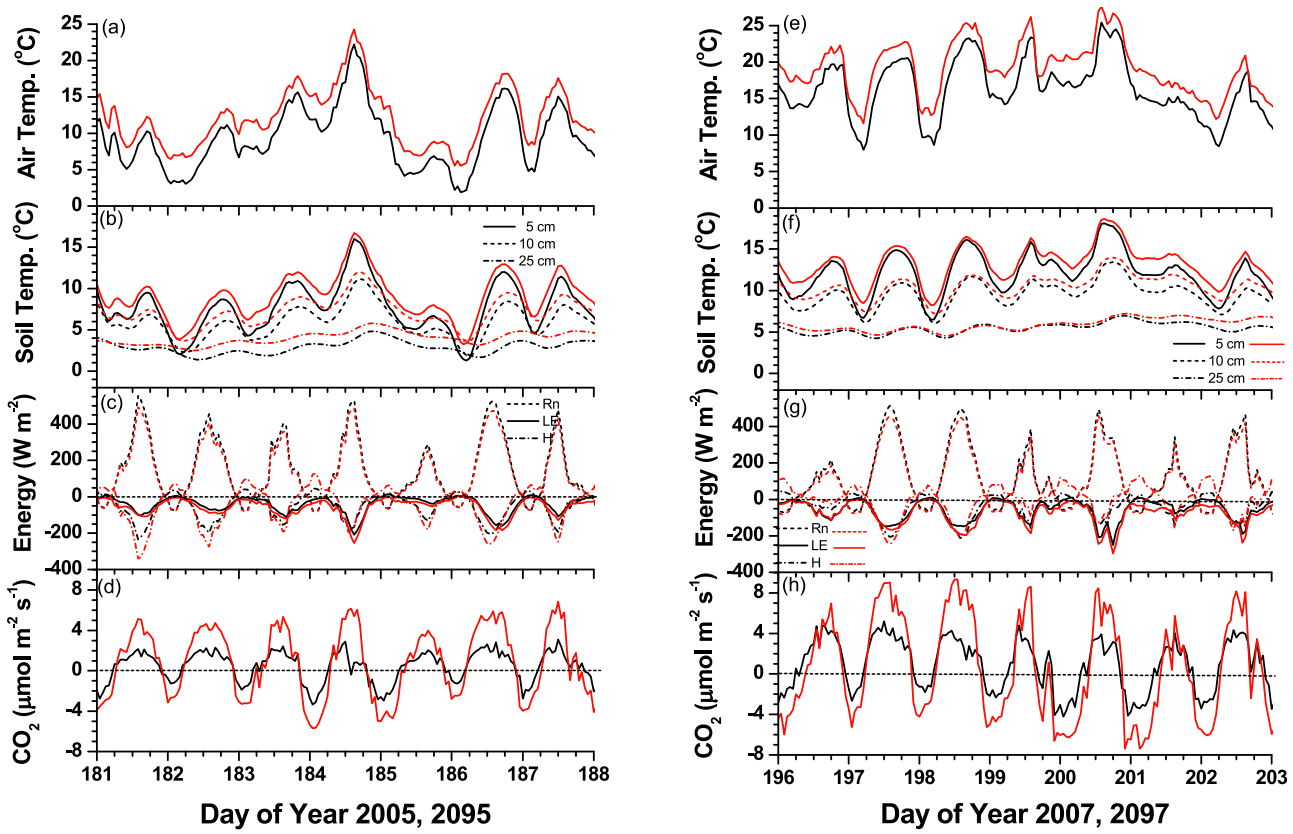

Figure 7. (a, e) Air temperatures recorded during DOY 182 to 188 in 2005 and DOY 197 to 203 in 2007 (black lines) and altered after 90 years (red lines) during a 150 year model run under climate change predicted by the Canadian Regional Circulation Model (CRCM) version 4.2 grid cell within which the Daring Lake site is located (see Table 2), (b, f) soil temperatures, (c, g) energy fluxes, and (d, h) CO_2 fluxes modeled during 182 to 188 in 2005 and DOY 197 to 203 in 2007 under current climate (black lines) and after 90 years of transient climate change (red lines).

also rose with C_a during climate change [C6], but R_h and R_a rose in relation to CO_2 fixation from greater warming during nights than days (Table 2 and Figures 7a and 7e). More intense warming events could therefore adversely affect NEP as climate change progresses.

[37] Greater net C uptake with climate change modeled during the growing season was partially offset by greater net C losses modeled during the rest of the year (Figure 6). These greater losses were caused by more rapid R_h driven by greater litterfall from increased NPP, and by soil warming (Figure 5c), particularly during early winters under deeper snowpacks (Figure 5a) when warming was greatest. However, gains in net C uptake exceeded those in net C losses, so that average annual NEP rose with climate change (Figure 6), as proposed in hypothesis 4. However, the adverse effects of warming on NEP also rose with climate change, causing increases in interannual variability of NEP.

[38] Annual R_h and NPP modeled under current climate rose gradually with C_a prior to the onset of climate change in model year 2009 (Figure 9a) while annual NEP remained stable (Figure 9b), indicating that the CO_2 exchange in the model had achieved equilibrium under the 4 year hourly weather record available at the time of writing. Average NEP modeled before 2009 was influenced by the average T_a of −9.5°C during this 4 year weather record (Table 4), which was slightly warmer than the long-term average of −10°C to −12.5°C estimated for Daring Lake from historical weather data (Table 1). Model processes governing CO_2 exchange caused annual R_h and NPP approximately to double during the first 100 years of climate change from those modeled under current climate (Figure 9a). The contrasting responses of net CO_2 exchange to warming under lower versus higher T_a (e.g., Figure 7d versus Figure 7h) caused average annual NEP and its interannual variability to rise gradually from 30 ± 13 g C m^{-2} yr^{-1} modeled under current climate, to 38 ± 25, 49 ± 32, and 57 ± 40 g C m^{-2} yr^{-1} after 30, 60 and 90 years, respectively, of climate change (Figures 6 and 9b). However, when the CRCM climate change scenario (Table 2) was extrapolated for a further 60 years, rises in R_h gradually exceeded those in NPP (Figure 9a) as the adverse effects of high-temperature events on net CO_2 uptake (Figure 7h) became more frequent and intense. Consequently annual NEP and its interannual variability rose to 63 ± 70 g C m^{-2} yr^{-1} after 120 years but then declined to 44 ± 51 g C m^{-2} yr^{-1} after 150 years as proposed in hypothesis 5. This gradual rise in NEP caused slow gains in shrub, sedge and soil C stocks from those modeled under current climate (Figure 9c). However, CH_4 emissions rose from near zero modeled during the first 140 years of climate change to 0.5 ± 0.3 g C m^{-2} yr^{-1} modeled during the last 10 years of climate change, indicating that

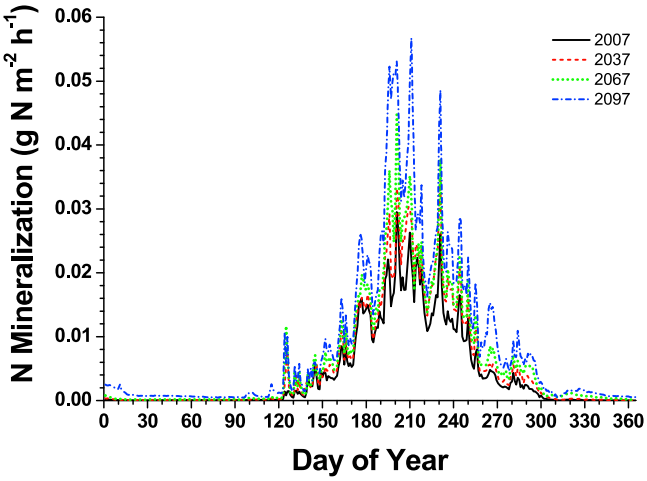

Figure 8. Daily N mineralization rates modeled during 2007 and at 30 year intervals thereafter from a continuous 150 year model run under repeating sequences of weather data recorded at Daring Lake from 1 January 2004 to 31 December 2007. These weather data were altered hourly during model years 2008 to 2157 according to climate change predicted by the Canadian Regional Circulation Model (CRCM) version 4.2 grid cell within which the Daring Lake site is located (see Table 2).

rising T_a and precipitation may eventually cause CH_4 emissions even in these mesic tundra sites.

4. Discussion

4.1. Modeled Versus Measured Fluxes

[39] Well-constrained tests of modeled ecosystem behavior under current climate are vital to support projections of ecosystem behavior under future climates. Such tests are enabled by *ecosys*' hourly time step, allowing direct use of partial differential equations parameterized from basic research that represent highly nonlinear responses of key ecosystem processes involved in C, N, water and heat transfers to diurnal changes in environment (see Text S1). The use of these equations permits well-constrained tests of *ecosys* directly against experimental measurements of these processes as they respond to hourly changes in weather (e.g., EC CO_2 and energy fluxes recorded under changing T_a and T_s in Table 3 and Figures 2 and 3). *Ecosys* thereby avoids assumptions required for temporally aggregating these responses to daily or monthly time scales in models used in earlier climate change studies that operate at longer time steps. These longer time steps permit less well-constrained tests against temporally aggregated flux measurements at daily or monthly time scales that require assumptions (e.g., gap filling) to which aggregated values are sensitive. The model tests against hourly fluxes indicated that most of the variation in CO_2 and energy fluxes measured by EC from 2004 through 2007 was explained without major bias by the model hypotheses implemented through the equations in the appendices, and that most of the remaining variation could be attributed to uncertainty estimated in the measured fluxes (Table 3). Tests of these modeled responses to short-term changes in weather supported the modeled responses to long-term changes in climate (Figures 5–7) that formed the basis of the climate change projections (Figure 9).

4.2. NEP Under Current Climate

[40] The rapid rise in NEP modeled and measured during June and early July after snowmelt, thawing and deciduous leafout (Figures 1c, 1f, 1i, and 1l) appears to be widely characteristic of arctic ecosystems [*Welker et al.*, 2004]. This rise was driven by CO_2 exchange during long days with intermediate irradiance, moderate T_a (<20°C) (Figures 2a, 2e, and 2i) and cool soils (Figures 2b, 2f, and 2j). Daily incoming shortwave radiation during this period reached 27–30 MJ m^{-2} d^{-1}, comparable to values in temperate ecosystems. Under these conditions, warming increased C uptake from GPP (Figures 2d, 2h, and 2l) more than C emissions from R_a and R_h, causing NEP to rise. The subsequent decline in NEP modeled and measured during later July and August (Figures 1c, 1f, 1i, and 1l) was driven by CO_2 exchange during shortening days with higher T_a (Figures 3a, 3e, and 3i) and T_s (Figures 3b, 3f, and 3j) when R_a and R_h increased relative to GPP, particularly when $T_a > 20$°C (Figures 3d, 3h, and 3l).

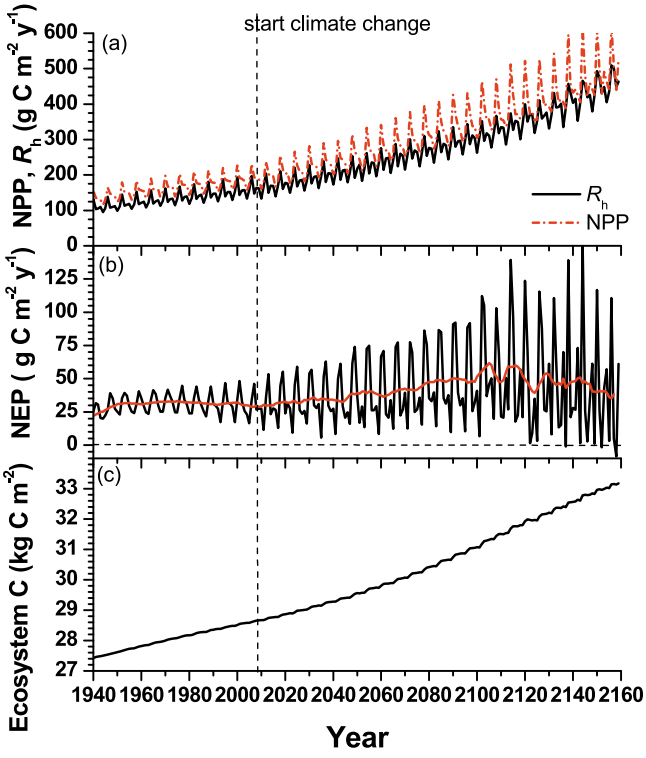

Figure 9. (a) Heterotrophic respiration (R_h), net primary productivity (NPP), (b) net ecosystem productivity (NEP) and its running average, and (c) ecosystem C modeled during a continuous 150 year model run under repeating sequences of weather data recorded at Daring Lake from 1 January 2004 to 31 December 2007. These weather data were altered hourly during model years 2008 to 2157 according to climate change predicted by the Canadian Regional Circulation Model (CRCM) version 4.2 grid cell within which the Daring Lake site is located (see Table 2).

[41] The timing of these rises and declines in NEP varied among years with the timing of spring thaw and autumn freezing. Net C uptake modeled (measured) during the growing season at Daring Lake rose from 47 (32) and 41 (51) g C m^{-2} in 2004 and 2005 to 59 (61) g C m^{-2} in 2006 when spring thaw advanced from DOY 162 and 155 to DOY 133 and autumn freezing was delayed from DOY 262 and 259 to DOY 272 (Table 4). However, net C uptake rose further to 76 (66) g C m^{-2} in 2007 when spring thaw was delayed to DOY 150 and autumn freezing advanced to DOY 258 (Table 4) because the growing season remained warm (Table 4) and because R_h declined with drying of surface litter and soil (e.g., Figure 2l). There may not therefore be a simple relationship between growing season length and NEP. In the model, rises in net C uptake from 2004 to 2007 were driven by greater rises in NPP than in R_h (Table 4), supporting hypotheses (1) that annual NPP and R_h of mesic arctic tundra both increase in years with earlier spring warming and snowmelt and decrease in those with later and (2) that interannual variability in NPP caused by earlier or later warming or cooling is greater than that in R_h and so drives interannual variability in NEP.

[42] Interannual variation in growing season length has been related to that in seasonal NEP in earlier studies of arctic and subarctic ecosystems. *Aurela et al.* [2001] attributed interannual variation in NEP from 74 to 207 g C m^{-2} yr^{-1} at a subarctic mountain birch stand to interannual variation in the timing of spring warming. Similarly *Aurela et al.* [2004] attributed interannual variation in NEP from 4 to 53 g C m^{-2} yr^{-1} at a subarctic fen to interannual variation in the timing of snowmelt. In both studies, interannual variation in GPP was greater than in R_e, and hence drove that in NEP, as modeled at Daring Lake from hypothesis 2 (Table 4). In both studies, seasonal variation in NEP was greatest during the first month of net C uptake, as also measured and modeled at Daring Lake (Figure 1). Similar responses of growing season NEP to variation in growing season length have also been reported by *Groendahl et al.* [2007] for a high arctic heath.

[43] Interannual variation in growing season length is probably better correlated with that in NPP. At a regional scale, *Kimball et al.* [2006] attributed gains of 1% or 2.4 g C m^{-2} yr^{-1} in NPP derived from a simple production model to 1 day advances in dates of spring thaw detected from satellite microwave imagery over arctic tundra in Alaska and northwestern Canada between 1988 and 2000. Such gains were consistent with those modeled over the mixed tundra at Daring Lake from 2004 to 2007 in which NPP rose by 2.9 g C m^{-2} yr^{-1} for each 1 day advance in the start of spring thaw ($R^2 = 0.98$) (Table 4). However, R_h modeled at Daring Lake rose by 2.3 g C m^{-2} yr^{-1} for each 1 day advance in the start of spring thaw ($R^2 = 0.92$) (Table 4). Annual R_h also rose sharply with delayed autumn freezing in 2006 (Table 4), as inferred at a regional scale from seasonal measurements of C_a and CO_2 fluxes by *Piao et al.* [2008]. Although a gain in NEP of 0.6 g C m^{-2} yr^{-1} d^{-1} advance in spring thaw was modeled in this study, the correlation between NEP and spring thaw was not significant ($R^2 = 0.28$).

[44] The adverse effects of short-term warming events on NEP at Daring Lake (Figures 3 and 4) as proposed in hypothesis 3 have also been found in other continental arctic ecosystems. *Kwon et al.* [2006] attributed increases in net C emission measured over a moist tussock tundra when T_a > 20°C [*Kwon et al.*, 2006, Figure 7] to increases in R_e with soil warming, and to decreases in GPP with lower g_s under higher D. The adverse effects of short-term warming events on NEP have also been found consistently in boreal forests [*Grant et al.*, 2008, 2009]. However, these adverse effects were less apparent in arctic coastal wetlands where R_h is limited by soil wetness [*Kwon et al.*, 2006], and not found in high arctic tundra where T_a currently does not exceed 20°C [e.g., *Groendahl et al.*, 2007; *Welker et al.*, 2004].

[45] Net C uptake modeled during the growing season at Daring Lake was largely offset by net C losses during the rest of the year (Figure 1) which varied from 24 to 31 g C m^{-2} yr^{-1} during 2004–2007 (Table 4). The interannual variation in net C losses was smaller than that in net C uptake as has been found experimentally elsewhere [e.g., *Aurela et al.*, 2004], supporting hypothesis 2. Total C losses of 31 g C m^{-2} modeled from 13 September 2004 to 18 June 2005 (Figures 1c and 1f) were close to an ecosystem respiration of 27 g C m^{-2} measured with surface flux chambers over the same period at Daring Lake by *Nobrega and Grogan* [2007].

4.3. NEP Under Climate Change

[46] The model projected substantial rises in NPP and R_h (Figure 9a), and hence small rises in NEP (Figure 9b) with lengthening growing seasons during climate change, as indicated in hypothesis 4. The model on which these projections were based included processes for the effects of rising T_a on T_s (Figure 5c), and thereby on the duration and depth of the soil active layer, and on R_h and net N mineralization (Figure 8). The model also included processes for the effects of rising C_a on GPP (Figures 7d and 7h), transpiration (Figures 7c and 7g), and hence on soil and plant water status, and for the effects of rising precipitation on snowpack depth (Figure 5a), and hence on θ and T_s (Figures 5b and 5c). This model thereby considered many of the processes either omitted or not fully considered in earlier modeling studies [*Qian et al.*, 2010; *Sitch et al.*, 2007] that are thought to govern climate change impacts on arctic tundra ecosystems.

[47] N transformations were among the most important of these processes. In the model, more rapid net N mineralization (Figure 8) driven by more rapid R_h in warmer, wetter soils (Figures 5b and 5c) enabled more rapid root N uptake and hence greater accumulation of root nonstructural N reserves. These greater reserves drove greater N transfer to leaves that enabled rises in modeled NPP which matched or exceeded those in R_h for the first 100 years under climate change (Figure 9a). The coupling of N uptake with NPP in *ecosys* is described and tested more fully by *Grant et al.* [2010b]. The sharp rises in net N mineralization, and hence in plant N uptake, modeled with warming in this study were consistent with results from several incubation studies of arctic soils in which small increases in T_s caused substantial increases in rates of N mineralization and uptake. For example, *Jonasson et al.* [2004] found that plant N uptake from a tundra heath soil approximately doubled with a rise in T_s from 10°C to 12°C, consistent with the increase in net N mineralization (Figure 8) modeled here in response to a similar rise in T_s over 90 years (Figure 7f).

[48] Soil R_h and net N mineralization were further hastened during climate change in the model by increasing

winter precipitation (Table 2) and consequently deeper snowpacks (Figure 5a), the insulating effects of which raised winter T_s (Figure 5c) more than might be predicted from climate warming alone. Rises in winter T_s and C emissions (Figure 6) with snowpack depth in the model were consistent with those measured in snow manipulation experiments at Daring Lake [*Nobrega and Grogan*, 2007]. Consequent rises in net N mineralization (Figure 8) were consistent with experimental evidence that deeper snowpacks and higher winter T_s increase early winter N mineralization and thereby alter the amount and timing of plant-available N in tundra ecosystems [*Schimel et al.*, 2004]. These model and experimental results indicate the importance of a fully coupled N cycle in models used to project climate change effects on arctic tundra productivity.

[49] Observations from which we can corroborate model projections of climate change impacts on tundra NEP are limited to those from artificial warming studies using OTC, greenhouses or infrared radiation. OTC warming by 1°C–2° C across diverse tundra sites raised R_e, particularly at drier sites, and usually raised GPP, particularly early in the growing season [*Oberbauer et al.*, 2007] as modeled in our study (Figure 6). Differences between rises in GPP and R_e with OTC warming varied among sites, such that NEP was usually, but not always, raised at moist sites where R_h was limited by soil aeration, and reduced at dry sites where GPP may have been limited by soil drying [*Oberbauer et al.*, 2007]. Warming of tussock tundra from 8°C to 15°C in an indoor greenhouse [*Johnson et al.*, 1996] and by 4°C above ambient in an outdoor greenhouse [*Hobbie and Chapin*, 1998] gave large but similar rises in both GPP and R_e, with little effect on NEP.

[50] However findings from OTC and greenhouse experiments would not fully account for the long-term effects of elevated C_a on GPP and ET, nor those of soil warming on N cycling. Enhanced N mineralization from warmed tundra soils has been found to alleviate nutrient constraints, enabling a sustained rise in GPP under elevated CO_2 [*Oechel et al.*, 1994], as modeled in our study (Figure 9a). Infrared warming of both vegetation and soil by 2.5°C in a high arctic tundra gave a rise in growing season GPP of 24%, partly attributed to a late season extension of net C uptake [*Marchand et al.*, 2004] as modeled in our study (Figure 6). This rise exceeded that in R_e, causing a small gain in NEP as well as in plant cover. The full effects of warming on NPP may also be inferred from changes in aboveground C (AGC) measured at sites where natural warming is already in progress. *Hudson and Henry* [2009] measured increases in AGC of 260% at a "polar oasis" on Ellesmere Island in response to a warming of approximately 2°C from 1981 to 2008. This increase is comparable to that in NPP modeled in response to similar warming over 90 years at Daring Lake (Figure 9a).

[51] Modeled rises in NPP were eventually exceeded by those in R_h after more than 100 years of climate change (Figure 9a), causing a gradual decline in NEP thereafter (Figure 9b) as proposed in hypothesis 5. This model finding required an extrapolation of changes in C_a, radiation, temperature and precipitation beyond the 90 years for which these changes were predicted (Table 2) and so can be stated with less confidence than model findings within the first 90 years. However, this decline in NEP indicated that rises in tundra C storage under climate change (Figure 9c) are not likely to continue indefinitely, but may end at some point in the future, depending on the climate change scenario.

[52] The model projections in our study build upon those of earlier studies with models that included fully coupled N cycles. In these studies, large but commensurate rises in decadally averaged NPP and R_h over 100 years of climate warming caused little change in decadally averaged NEP of a coastal wet sedge tundra [*Grant et al.*, 2003] and of sedge and shrub tundras [*Euskirchen et al.*, 2009] in northern Alaska. However, our projections differ from those of other studies with models that did not include N cycles in which NEP of northern high latitudes rose until *ca*. 2060 but declined thereafter, approaching zero by 2100 [*Qian et al.*, 2010].

[53] We should note that our model projections of NEP at Daring Lake did not account for effects of disturbances such as grazing or fire, although such disturbances are currently rare. Increased fire frequency would substantially reduce the rises in NEP modeled with increased woody biomass under climate change [e.g., *Zhuang et al.*, 2006]. Future projections should include the adverse effects of fire on ecosystem C stocks, both directly through combustion (as in the work by *Grant et al.* [2006]), and indirectly through subsequent exposure, warming and accelerated decomposition (as in the work by *Grant et al.* [2010a]). These projections should also be made under some alternative climate change scenarios to evaluate a range of possible impacts on tundra productivity.

5. Conclusions

[54] Three hypotheses for ecological controls on NEP of a mesic arctic tundra were supported by model tests in this study.

[55] 1. Annual NPP and R_h of a mesic arctic tundra both rose in warmer years with longer growing seasons and declined in cooler years with shorter growing seasons (Table 4).

[56] 2. Interannual variability in NPP was larger than that in R_h and so caused NEP to rise in warmer years and to decline in cooler (Table 4).

[57] 3. Midseason warming events (T_a > 20°C) raised R_h more than NPP and thereby briefly lowered NEP (Figures 1, 3, and 4).

[58] Changes in NPP and R_h arising from these hypotheses supported two further hypothesis based on model projections of NEP under climate change.

[59] 4. NPP, R_h, and their interannual variabilities increased with warming during the first 100 years of climate change (Figure 9a), causing rises in NEP and its interannual variability (Figure 9b), consistent with hypotheses 1 and 2. These greater rises in NPP were largely driven by more rapid N mineralization with more rapid R_h in warming soil (Figure 8).

[60] 5. However, rises in R_h gradually exceeded those in NPP after more than 100 years of climate change (Figure 9a) as midseason warming events became more frequent and intense (Figure 7), causing NEP to decline (Figure 9b) consistent with hypothesis 3.

[61] **Acknowledgments.** Computing facilities for *ecosys* were provided by the University of Alberta and by Cybera, a corporation managing cyberinfrastructure-related technologies in collaboration with academic and

industry partners. Funding for the work at Daring Lake was provided by grant 2006-SR1-CC-096 from the Government of Canada Program for International Polar Year. Earlier (2004–2006) support for the Daring Lake field measurement program to P.M.L. and E.R.H. was provided by the Canadian Foundation for Climate and Atmospheric Sciences. P.M.L. and E.R.H. thank the manager (Steve Matthews) and staff of the Daring Lake Terrestrial Ecology Research Station for logistical support throughout the measurement campaigns.

References

Aurela, M., J.-P. Tuovinen, and T. Laurila (2001), Net CO_2 exchange of a subarctic mountain birch ecosystem, *Theor. Appl. Climatol.*, *70*, 135–148, doi:10.1007/s007040170011.

Aurela, M., T. Laurila, and J.-P. Tuovinen (2004), The timing of snow melt controls the annual CO_2 balance in a subarctic fen, *Geophys. Res. Lett.*, *31*, L16119, doi:10.1029/2004GL020315.

Chapin, F. S., III, and G. R. Shaver (1996), Physiological and growth responses of arctic plants to a field experiment simulating climatic change, *Ecology*, *77*, 822–840, doi:10.2307/2265504.

Chapin, F. S., III, G. R. Shaver, A. E. Giblin, K. J. Nadelhoffer, and J. A. Laundre (1995), Responses of arctic tundra to experimental and observed changes in climate, *Ecology*, *76*, 694–711, doi:10.2307/1939337.

Christensen, T. R., I. C. Prentice, J. Kaplan, A. Haxeltine, and S. Sitch (1996), Methane flux from northern wetlands and tundra: An ecosystem source modelling approach, *Tellus, Ser. B*, *48*, 652–661, doi:10.1034/j.1600-0889.1996.t01-4-00004.x.

Climatic Atlas of Canada (1984), *Map Series 1 and 2*, Gov. of Can., Ottawa, Ont.

Dredge, L. A., D. E. Kerr, and S. A. Wolfe (1999), Surficial materials and related ground ice conditions, Slave Province, N.W.T., Canada, *Can. J. Earth Sci.*, *36*, 1227–1238, doi:10.1139/cjes-36-7-1227.

Euskirchen, E. S., A. D. McGuire, F. S. Chapin III, S. Yi, and C. C. Thompson (2009), Changes in vegetation in northern Alaska under scenarios of climate change, 2003–2100: Implications for climate feedbacks, *Ecol. Appl.*, *19*, 1022–1043, doi:10.1890/08-0806.1.

Fahnestock, J. T., M. H. Jones, and J. M. Welker (1999), Wintertime CO_2 efflux from Arctic soils: Implications for annual carbon budgets, *Global Biogeochem. Cycles*, *13*(3), 775–779, doi:10.1029/1999GB900006.

Grant, R. F. (2001), A review of the Canadian ecosystem model *ecosys*, in *Modeling Carbon and Nitrogen Dynamics for Soil Management*, edited by M. Shaffer, pp. 173–263, CRC Press, Boca Raton, Fla.

Grant, R. F., and L. B. Flanagan (2007), Modeling stomatal and nonstomatal effects of water deficits on CO_2 fixation in a semiarid grassland, *J. Geophys. Res.*, *112*, G03011, doi:10.1029/2006JG000302.

Grant, R. F., and I. A. Nalder (2000), Climate change effects on net carbon exchange of a boreal aspen-hazelnut forest: Estimates from the ecosystem model *ecosys*, *Global Change Biol.*, *6*, 183–200, doi:10.1046/j.1365-2486.2000.00288.x.

Grant, R. F., and N. T. Roulet (2002), Methane efflux from boreal wetlands: Theory and testing of the ecosystem model *ecosys* with chamber and tower flux measurements, *Global Biogeochem. Cycles*, *16*(4), 1054, doi:10.1029/2001GB001702.

Grant, R. F., R. L. Garcia, P. J. Pinter Jr., D. Hunsaker, G. W. Wall, B. A. Kimball, and R. L. LaMorte (1995a), Interaction between atmospheric CO_2 concentration and water deficit on gas exchange and crop growth: Testing of *ecosys* with data from the Free Air CO_2 Enrichment (FACE) experiment, *Global Change Biol.*, *1*, 443–454, doi:10.1111/j.1365-2486.1995.tb00042.x.

Grant, R. F., B. A. Kimball, P. J. Pinter Jr., G. W. Wall, R. L. Garcia, R. L. LaMorte, and D. J. Hunsaker (1995b), CO_2 effects on crop energy balance: Testing *ecosys* with a Free Air CO_2 Enrichment (FACE) experiment, *Agron. J.*, *87*, 446–457, doi:10.2134/agronj1995.00021962008700030010x.

Grant, R. F., G. W. Wall, K. F. A. Frumau, P. J. Pinter Jr., D. Hunsaker, B. A. Kimball, and R. L. LaMorte (1999), Crop water relations under different CO_2 and irrigation: Testing of *ecosys* with the Free Air CO_2 Enrichment (FACE) experiment, *Agric. For. Meteorol.*, *95*, 27–51, doi:10.1016/S0168-1923(99)00017-9.

Grant, R. F., et al. (2001), CO_2 effects on mass and energy exchange of wheat under different N fertilization: Model theory and testing with a Free Air CO_2 Enrichment (FACE) experiment, *Agron. J.*, *93*, 638–649, doi:10.2134/agronj2001.933638x.

Grant, R. F., W. C. Oechel, C. Ping, and H. Kwon (2003), Carbon balance of coastal arctic tundra under changing climate, *Global Change Biol.*, *9*, 16–36, doi:10.1046/j.1365-2486.2003.00549.x.

Grant, R. F., et al. (2004), How elevated CO_2 affects water relations, water use and growth of irrigated sorghum: Testing a model with results from a Free Air CO_2 Enrichment (FACE) experiment, *Agron. J.*, *96*, 1693–1705, doi:10.2134/agronj2004.1693.

Grant, R. F., T. A. Black, D. Gaumont-Guay, N. Kljun, A. G. Barr, K. Morgenstern, and Z. Nesic (2006), Net ecosystem productivity of boreal aspen forests under drought and climate change: Mathematical modelling with *ecosys*, *Agric. For. Meteorol.*, *140*, 152–170, doi:10.1016/j.agrformet.2006.01.012.

Grant, R. F., et al. (2007a), Net ecosystem productivity of boreal jack pine stands regenerating from clearcutting under current and future climates, *Global Change Biol.*, *13*, 1423–1440, doi:10.1111/j.1365-2486.2007.01363.x.

Grant, R. F., T. A. Black, E. R. Humphreys, and K. Morgenstern (2007b), Changes in net ecosystem productivity with forest age following clearcutting of a coastal Douglas fir forest: Testing a mathematical model with eddy covariance measurements along a forest chronosequence, *Tree Physiol.*, *27*, 115–131.

Grant, R. F., H. A. Margolis, A. G. Barr, T. A. Black, A. L. Dunn, P. Y. Bernier, and O. Bergeron (2008), Changes in net ecosystem productivity of boreal black spruce stands in response to changes in temperature at diurnal and seasonal time scales, *Tree Physiol.*, *29*, 1–17, doi:10.1093/treephys/tpn004.

Grant, R. F., A. G. Barr, T. A. Black, H. A. Margolis, A. L. Dunn, J. Metsaranta, S. Wang, J. H. McCaughey, and C. P.-A. Bourque (2009), Interannual variation in net ecosystem productivity of Canadian forests as affected by regional weather patterns—A Fluxnet-Canada synthesis, *Agric. For. Meteorol.*, *149*, 2022–2039, doi:10.1016/j.agrformet.2009.07.010.

Grant, R. F., A. G. Barr, T. A. Black, H. A. Margolis, J. H. McCaughey, and J. A. Trofymow (2010a), Net ecosystem productivity of temperate and boreal forests after clearcutting—A Fluxnet-Canada measurement and modelling synthesis, *Tellus, Ser. B*, *62*, 475–496, doi:10.1111/j.1600-0889.2010.00500.x.

Grant, R. F., T. A. Black, R. S. Jassal, and C. Bruemmer (2010b), Changes in net ecosystem productivity and greenhouse gas exchange with fertilization of Douglas fir: Mathematical modeling in *ecosys*, *J. Geophys. Res.*, *115*, G04009, doi:10.1029/2009JG001094.

Groendahl, L., T. Friborg, and H. Soegaard (2007), Temperature and snowmelt controls on interannual variability in carbon exchange in the high Arctic, *Theor. Appl. Climatol.*, *88*, 111–125, doi:10.1007/s00704-005-0228-y.

Hayne, S. (2009), Controls on atmospheric exchanges of carbon dioxide and methane for a variety of arctic tundra types, M.Sc. thesis, 157 pp., Dep. of Geogr. and Environ. Stud., Carleton Univ., Ottawa, Ont.

Hobbie, S. E., and F. S. Chapin (1998), The response of tundra plant biomass, aboveground production, nitrogen and CO_2 flux to experimental warming, *Ecology*, *79*, 1526–1544.

Hudson, J. M. G., and G. H. R. Henry (2009), Increased plant biomass in a High Arctic heath community from 1981 to 2008, *Ecology*, *90*, 2657–2663, doi:10.1890/09-0102.1.

Johnson, L. C., G. R. Shaver, A. E. Giblin, K. J. Nadelhoffer, E. R. Rastetter, J. A. Laundre, and G. L. Murray (1996), Effects of drainage and temperature on carbon balance of tussock tundra ecosystems, *Oecologia*, *108*, 737–748, doi:10.1007/BF00329050.

Jonasson, S., J. Castro, and A. Michelsen (2004), Litter, warming and plants affect respiration and allocation of soil microbial and plant C, N and P in arctic mesocosms, *Soil Biol. Biochem.*, *36*, 1129–1139, doi:10.1016/j.soilbio.2004.02.023.

Kimball, J. S., K. C. McDonald, and M. Zhao (2006), Spring thaw and its effect on terrestrial vegetation productivity in the western arctic observed from satellite microwave and optical remote sensing, *Earth Interact.*, *10*, 1–22, doi:10.1175/EI187.1.

Kwon, H.-J., W. C. Oechel, R. C. Zulueta, and S. J. Hastings (2006), Effects of climate variability on carbon sequestration among adjacent wet sedge tundra and moist tussock tundra ecosystems, *J. Geophys. Res.*, *111*, G03014, doi:10.1029/2005JG000036.

Lafleur, P. M., and E. R. Humphreys (2008), Spring warming and carbon dioxide exchange over low Arctic tundra in central Canada, *Global Change Biol.*, *14*, 740–756, doi:10.1111/j.1365-2486.2007.01529.x.

Laurila, T., H. Soegaard, C. R. Lloyd, M. Aurela, J.-P. Tuovinen, and C. Nordstroem (2001), Seasonal variation of net CO_2 exchange in European arctic ecosystems, *Theor. Appl. Climatol.*, *70*, 183–201, doi:10.1007/s007040170014.

Li, T., R. F. Grant, and L. B. Flanagan (2004), Climate impact on net ecosystem productivity of a semi-arid natural grassland: Modeling and measurement, *Agric. For. Meteorol.*, *126*, 99–116, doi:10.1016/j.agrformet.2004.06.005.

Lloyd, C. R. (2001), The measurement and modelling of the carbon dioxide exchange at a high Arctic site in Svalbard, *Global Change Biol.*, *7*, 405–426, doi:10.1046/j.1365-2486.2001.00422.x.

Marchand, F. L., I. Nijs, H. J. de Boeck, F. Kockelbergh, and S. Martens (2004), Increased turnover but little change in the carbon balance of a

high arctic tundra exposed to whole growing season warming, *Arct. Antarct. Alp. Res.*, *36*, 298–307, doi:10.1657/1523-0430(2004)036[0298:ITBLCI]2.0.CO;2.

McGuire, A. D., L. G. Anderson, T. R. Christensen, S. Dallimore, L. Guo, D. J. Hayes, M. Heimann, T. D. Lorenson, R. W. Macdonald, and N. Roulet (2009), Sensitivity of the carbon cycle in the Arctic to climate change, *Ecol. Monogr.*, *79*, 523–555, doi:10.1890/08-2025.1.

Meteorological Service of Canada (2004), *Canadian Acid Deposition Science Assessment*, Environ. Can., Ottawa, Ont.

Music, B., and D. Caya (2007), Evaluation of the hydrological cycle over the Mississippi River Basin as simulated by the Canadian Regional Climate Model (CRCM), *J. Hydrometeorol.*, *8*(5), 969–988, doi:10.1175/JHM627.1.

Nobrega, S., and P. Grogan (2007), Deeper snow enhances winter respiration from both plant-associated and bulk soil carbon pools in birch hummock tundra, *Ecosystems*, *10*, 419–431, doi:10.1007/s10021-007-9033-z.

Nobrega, S., and P. Grogan (2008), Landscape and ecosystem-level controls on net carbon dioxide exchange along a natural moisture gradient in Canadian low arctic tundra, *Ecosystems*, *11*, 377–396, doi:10.1007/s10021-008-9128-1.

Oberbauer, S. F., et al. (2007), Tundra CO_2 fluxes in response to experimental warming across latitudinal and moisture gradients, *Ecol. Monogr.*, *77*, 221–238, doi:10.1890/06-0649.

Oechel, W. C., and G. L. Vourlitis (1994), The effects of climate change on arctic tundra ecosystems, *Trends Ecol. Evol.*, *9*, 324–329, doi:10.1016/0169-5347(94)90152-X.

Oechel, W. C., S. Cowles, N. Grulke, S. J. Hastings, B. Lawrence, T. Prodhomme, G. Reichers, B. Strain, D. Tissue, and G. Vourlitis (1994), Transient nature of CO_2 fertilization in arctic tundra, *Nature*, *371*, 500–503, doi:10.1038/371500a0.

Oechel, W. C., G. Vourlitis, and S. J. Hastings (1997), Cold season CO_2 emission from Arctic soils, *Global Biogeochem. Cycles*, *11*(2), 163–172, doi:10.1029/96GB03035.

Piao, S., et al. (2008), Net carbon dioxide losses of northern ecosystems in response to autumn warming, *Nature*, *451*, 49–52, doi:10.1038/nature06444.

Polyakov, I. V., G. V. Alekseev, R. V. Bekryaev, U. Bhatt, R. L. Colony, M. A. Johnson, V. P. Karklin, A. P. Makshtas, D. Walsh, and A. V. Yulin (2002), Observationally based assessment of polar amplification of global warming, *Geophys. Res. Lett.*, *29*(18), 1878, doi:10.1029/2001GL011111.

Qian, H., R. Joseph, and N. Zeng (2010), Enhanced terrestrial carbon uptake in the northern high latitudes in the 21st century from the Coupled Carbon Cycle Climate Model Intercomparison Project model projections, *Global Change Biol.*, *16*, 641–656, doi:10.1111/j.1365-2486.2009.01989.x.

Richardson, A. D., et al. (2006), A multi-site analysis of random error in tower-based measurements of carbon and energy fluxes, *Agric. For. Meteorol.*, *136*, 1–18, doi:10.1016/j.agrformet.2006.01.007.

Schimel, J. P., C. Bilbrough, and J. M. Welker (2004), Increased snow depth affects microbial activity and nitrogen mineralization in two Arctic tundra communities, *Soil Biol. Biochem.*, *36*, 217–227, doi:10.1016/j.soilbio.2003.09.008.

Sitch, S., A. D. Mcguire, J. Kimball, N. Gedney, J. Gamon, R. Engstrom, A. Wolf, Q. Zhuang, J. Clein, and K. C. Mcdonald (2007), Assessing the carbon balance of circumpolar arctic tundra using remote sensing and process modeling, *Ecol. Appl.*, *17*, 213–234, doi:10.1890/1051-0761(2007)017[0213:ATCBOC]2.0.CO;2.

Tarnocai, C., J. G. Canadell, G. Mazhitova, E. A. G. Schuur, P. Kuhry, and S. Zimov (2009), Soil organic carbon pools in the northern circumpolar permafrost region, *Global Biogeochem. Cycles*, *23*, GB2023, doi:10.1029/2008GB003327.

Waring, R. H., and S. W. Running (1998), *Forest Ecosystems: Analysis at Multiple Scales*, 2nd ed., Academic, San Diego, Calif.

Weintraub, M. N., and J. P. Schimel (2005), Nitrogen cycling and the spread of shrubs control changes in the carbon balance of Arctic tundra ecosystems, *BioScience*, *55*, 408–415, doi:10.1641/0006-3568(2005)055[0408:NCATSO]2.0.CO;2.

Welker, J. M., J. T. Fahnestock, G. H. R. Henry, K. W. O'Dea, and R. A. Chimner (2004), CO_2 exchange in three Canadian High Arctic ecosystems: Response to long-term experimental warming, *Global Change Biol.*, *10*, 1981–1995, doi:10.1111/j.1365-2486.2004.00857.x.

Wesely, M. L., and R. L. Hart (1985), Variability of short term eddy-correlation estimates of mass exchange, in *The Forest-Atmosphere Interaction*, edited by B. A. Hutchinson and B. B. Hicks, pp. 591–612, D. Reidel, Dordrecht, Netherlands.

Zhuang, Q., J. M. Melillo, M. C. Sarofin, D. W. Kicklighter, A. D. McGuire, B. S. Felzer, A. Sokolov, R. G. Prinn, P. A. Steudler, and S. Hu (2006), CO_2 and CH_4 exchanges between land ecosystems and the atmosphere in northern high latitudes over the 21st century, *Geophys. Res. Lett.*, *33*, L17403, doi:10.1029/2006GL026972.

D. D. Dimitrov, Canadian Forest Service, Edmonton, AB T6H 3S5, Canada.

R. F. Grant, Department of Renewable Resources, University of Alberta, Edmonton, AB T6G 2E3, Canada. (robert.grant@ales.ualberta.ca)

E. R. Humphreys, Department of Geography, Carleton University, Ottawa, ON K1S 5B6, Canada.

P. M. Lafleur, Department of Geography, Trent University, Peterborough, ON K9J 7B8, Canada.